

Article

# Simulation Optimization of Search and Rescue in Disaster Relief Based on Distributed Auction Mechanism

Jian Tang, Kejun Zhu \*, Haixiang Guo, Can Liao  and Shuwen Zhang

School of Economics and Management, China University of Geosciences, Wuhan 430074, China; tangjian@cug.edu.cn (J.T.); ghx@cug.edu.cn (H.G.); liaocan@cug.edu.cn (C.L.); zsw@cug.edu.cn (S.Z.)

\* Correspondence: zhukejun@cug.edu.cn

Received: 1 September 2017; Accepted: 12 November 2017; Published: 15 November 2017

**Abstract:** In this paper, we optimize the search and rescue (SAR) in disaster relief through agent-based simulation. We simulate rescue teams' search behaviors with the improved Truncated Lévy walks. Then we propose a cooperative rescue plan based on a distributed auction mechanism, and illustrate it with the case of landslide disaster relief. The simulation is conducted in three scenarios, including "fatal", "serious" and "normal". Compared with the non-cooperative rescue plan, the proposed rescue plan in this paper would increase victims' relative survival probability by 7–15%, increase the ratio of survivors getting rescued by 5.3–12.9%, and decrease the average elapsed time for one site getting rescued by 16.6–21.6%. The robustness analysis shows that search radius can affect the rescue efficiency significantly, while the scope of cooperation cannot. The sensitivity analysis shows that the two parameters, the time limit for completing rescue operations in one buried site and the maximum turning angle for next step, both have a great influence on rescue efficiency, and there exists optimal value for both of them in view of rescue efficiency.

**Keywords:** disaster relief; simulation optimization; Truncated Lévy walks; distributed auction mechanism; cooperative rescue

---

## 1. Introduction

Search and rescue of victims in large-scale disasters is of great importance in disaster relief. The research of disaster relief has focused mostly on emergency supplies reserves, location problems, emergency transportation, resource allocation and evacuation [1–7], which has provided an important theoretical foundation for disaster relief and improved rescue efficiency for sure. However, the research about search and rescue in the post-disaster phase are rarely seen.

The cooperation between rescue teams is essentially about task allocation. Many approaches for the task allocation problem have been proposed, such as contract net protocol [8,9], intelligent algorithm-based approaches [10–13] and auction-based approaches [14–16], etc.

Contract net protocol is a market-based approach that was proposed as early as 1980 [17]. Liang and Kang [8] have proposed an improved contract net protocol for task allocation in agent-oriented unmanned underwater vehicle (UUV) swarm system. Su et al. [9] employed contract net protocol for task allocation at an assembly point when adjusting group members periodically.

Intelligent algorithms are also frequently adopted in this problem. Ju and Chen [10] have applied the extended labor division model of ant colony to task allocation in a dynamic environment. Liu and Kroll [11] have developed a novel memetic algorithm for multi-robot task allocation of inspection problems.

One of the most used approaches is auction-based strategy. Nanjanath et al. [14] have used Sequential Single Item Auctions to assign tasks to agents. Nair et al. [15] have developed two

auction-based approaches, a centralized combinatorial auction mechanism and a distributed method. Kong et al. [16] have proposed a decentralized indicator-based combinatorial auction strategy for group task allocation.

Moreover, some task allocation problems have been solved through coalition formation. The sequential and holistic coalition methods proposed in [18] provided both online and offline solutions for task allocation into a group of heterogeneous mobile robots. Ramchurn et al. [19] have provided a DCOP formulation of the coalition problem and solve it with the Max-Sum algorithm.

In this paper, agent-based simulation is used to model the disaster relief. Compared with other approaches such as discrete event simulation [20,21], agent-based approach could describe the interaction between agents in complex systems. The agent-based approach is more appropriate to model complex systems and cope with the complexities and dynamics in complex systems [22]. In agent-based simulation, the conceptual model was built from the view of agents. Furthermore, the agents are autonomous [23], which means they can carry out some set of operations with some degree of independence or autonomy. The agents can react to the environment and act on it, while, in discrete event simulation (DES), the model was built from the view of event. The entities in the DES are not autonomous, and they cannot make decisions on their own. Thus, the entities' status cannot be decided by themselves.

There exist few researches which integrate search with cooperative rescue in disaster relief. However, search and rescue are inseparable in disaster relief. In this paper, we first construct a post-disaster environment based on multi-agent modeling. The survival probabilities of victims trapped in rubble are assumed to deteriorate with time [24]. Related to the search for victims, it has been proved that for randomly located targets, whether the targets can be revisited many times or not, and whether the targets are fixed or moving, Lévy walks is an efficient strategy [25,26]. In addition, Rhee et al. [27] have found that the patterns of human walks and Lévy walks are similar in some statistical properties. Thus, we adopt the improved Truncated Lévy walks [25] to simulate rescue teams' search behaviors. Finally, we propose a cooperative rescue plan based on distributed auction mechanism, evaluate its performance with the case of landslide rescue, and analyze its effect on rescue efficiency in different scenarios. The robustness and sensitivity of our proposed cooperative plan are tested as well.

The structure of the paper is organized as follows. Section 2 introduces the problem and describes two types of agent, victims and rescue teams. Section 3 introduces the cooperative rescue plan based on distributed auction mechanism. The simulations of the cooperative rescue plan are shown in Section 4. The robustness and sensitivity of our proposed cooperative plan are evaluated in Section 5. Conclusions are given in Section 6.

## 2. Description of Multi-Agent Model

In this paper, we have adopted a bottom-up approach to model the search and rescue (SAR). Before we built the conceptual model, we had gathered a lot of detailed information about SAR through the interviews carried out with first responders and experts who specialize in on-site search and rescue in disaster. In this model, shown in Figure 1, two types of active agents are defined, namely victims and rescue teams, and they can act upon their own initiative [28]. Apart from the active agents, there are passive agents in this model, such as the buried sites. The passive agents are solely reactive. The buried sites are spread randomly in the affected area, and they differ in buried depth. There might exist one or more victims in each site. The victim agents have a property, i.e., survival probability. Without timely rescue, the health condition of a victim could deteriorate continuously, thus the survival probability will decrease with time, and they may be dead as time passes. The rescue teams are agents that can take actions against disastrous situations. They can sense the environment, interact with other agents, and plan the next actions according to their objectives, such as searching for victims, rescuing a buried site, calling for cooperation and so on [23].

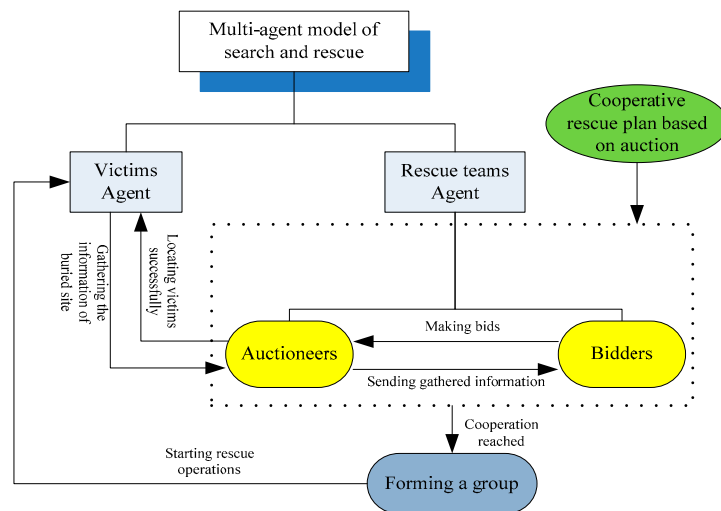


Figure 1. The model of multi-agent simulation.

The rescue teams search victims in the affected area, and if there are survivors trapped in a buried site within the search radius, rescue teams are able to locate the buried site with a certain probability. The rescue teams who locate the buried site take on the role of auctioneers, and other rescue teams who are not at work presently within the scope of cooperation take on the role of bidders. The interaction takes place mostly between rescue teams, which include auctioneers and bidders, and the interaction is carried out through communication. The communication is modeled as the input that agents receive and the outputs that they produce [28]. Auctioneers would communicate with bidders who are within the scope of cooperation if necessary, sending messages about victims’ coordinates, buried depth, etc. The bidders receive the auction messages, calculate the bids, and send them back to the auctioneers. Finally, the auctioneers will determine the winning bids, and send the message to bidders. The rescue operations would start once the cooperation is reached.

2.1. Victims

The essential parameters of victims include buried depth  $v_{rubble}$ , coordinates  $v_{xy}$  and injury severity  $v_{si}$ .

Buried depth  $v_{rubble}$  indicates the amount of rubble over the trapped victims. It is assumed that victims in the same buried site are equal in buried depth  $v_{rubble}$ . Coordinates  $v_{xy}$  indicate the location of victims.

Injury severity  $v_{si} \in \{“Death”, “Heavy injury”, “Slight injury”, “No injury”\}$ . Each victims’ injury severity will be decided by medical staff according to their mental status, respiration, etc. In this paper, three scenarios are assumed (“Fatal”, “Serious” and “Normal”), and they will be combined with injury severities.

2.2. Rescue Teams

The essential parameters of rescue teams include search radius  $s_r$ , maximum turning angle  $s_a$ , speed of rescue  $s_{rubble}$ , scope of cooperation  $s_c$ , move length  $s_l$ , turning angle  $s_\theta$ .

Search radius  $s_r$  indicates the maximum extent of the search for survivors. Maximum turning angle  $s_a$  indicates the range of turning angle in each step, shown in Figure 2. Speed of rescue  $s_{rubble}$  indicates speed of move rubbles by a rescue team. Scope of cooperation  $s_c$  indicates that the cooperation only occurs between rescue teams in this specified area.

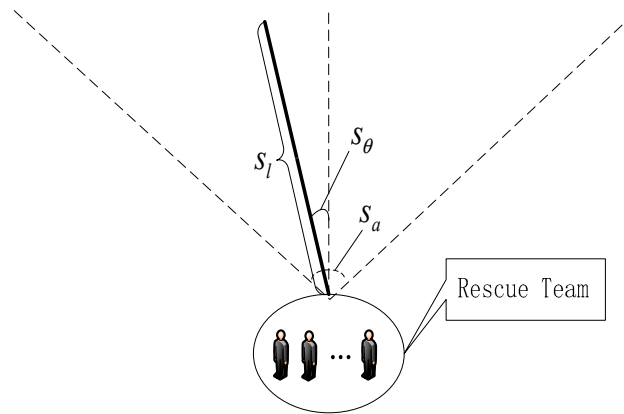


Figure 2. The movement of rescue teams.

In rescue teams’ searching process, shown in Figure 2, they move along the steps which are determined by move lengths  $s_l$  and turning angles  $s_\theta$ . The move length and turning angle are drawn from particular probability distributions. The steps are terminated when a move length or boundary is reached, or when a buried site is detected. At the end of a step, rescue teams move to the buried site or selects next step to continue searching [29].

Truncated Lévy walks are adopted to simulate rescue teams’ search behaviors in this paper [25]. The move lengths in Lévy walks are drawn from generalized Lévy probability density distribution:

$$P(s_l) = cs_l^{-\mu}, 1 < \mu \leq 3 \tag{1}$$

where  $c$  is a constant,  $\mu$  denotes Lévy index. In order to impose restrictions on move lengths, Truncated Lévy walks are adopted in the simulation. Thus, the probability density function of move length is

$$P(s_l) = \begin{cases} 0, & s_l > l_{\max} \\ \frac{\mu-1}{l_{\min}^{1-\mu} - l_{\max}^{1-\mu}} \times s_l^{-\mu}, & l_{\min} \leq s_l \leq l_{\max}, 1 < \mu \leq 3 \\ 0, & s_l < l_{\min} \end{cases} \tag{2}$$

where  $l_{\min}, l_{\max}$  denote the minimum and maximum move length, respectively. The buried sites within the search radius are possible to be detected by rescue teams; consequently, the move lengths are larger than  $l_{\min}$ , corresponding to the search radius of rescue teams. The move lengths are truncated at the distance  $l_{\max}$ , corresponding to limit scale of environment [25,30]. The corresponding sampling functions are obtained directly applying the Inverse Transform Sampling.

$$s_l = \left[ (l_{\max}^{1-\mu} - l_{\min}^{1-\mu})\gamma + l_{\min}^{1-\mu} \right]^{1/1-\mu}, \quad \gamma \sim U(0,1) \tag{3}$$

The turning angles in traditional Lévy walks are drawn from uniform distribution  $U(0, 2\pi)$ .

In this paper, turning angles  $s_\theta$  are drawn from uniform distribution  $U(0, s_a)$ , where  $s_a$  is used instead. The  $s_a$  shall be discussed later as a controllable parameter.

The searching plan of rescue teams is shown in Figure 3.

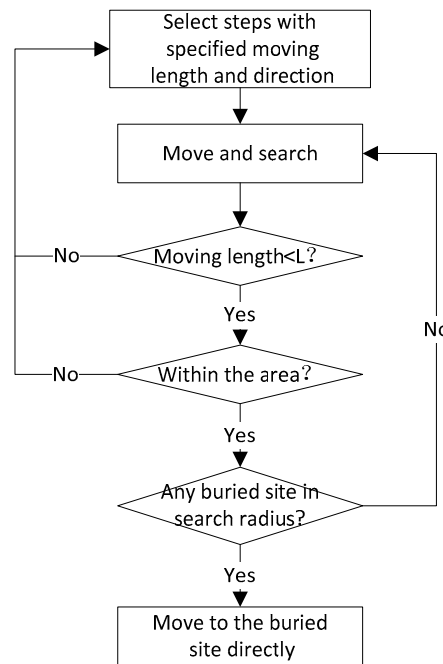


Figure 3. Searching plan of rescue teams.

### 3. Auction-Based Cooperative Rescue Plan

Auction is an efficient way to allocate resources, for its low information cost and high efficiency. It often takes place in economic activities. Bidders make bids on the item according to their evaluation of the item. Auctioneers allocate the item based on bidders’ bids.

The task allocation algorithm based on distributed auction mechanism will be adopted to allocate rescuing tasks between rescue teams within the scope of cooperation. The notations related to the auction-based algorithm are shown in Table 1. All teams are assumed to be equal in the rescue capability. When a number of teams work together as a coalition, the coalition’s speed of rescue would be the summation of  $s_{rubble}$  of all the teams in this coalition. There exist two types of role in the allocation, that is, task publisher  $A_i$  and task responder  $B_j$ , corresponding to the auctioneers and bidders in auction, respectively. The purpose of the auction-based algorithm is maximization of overall performance. In what follows, we detail how the rescue teams act to reach cooperation.

Table 1. Main notations related to the auction-based algorithm.

Notation	Definition
$N = \{1, 2, \dots, n\}$	The set of buried site, where $i \in N$ denotes a buried site
$M = \{1, 2, \dots, m\}$	The set of rescue teams, where $j \in M$ denotes a rescue team
$T_i$	The task of rescuing buried site $i$ , where $i \in N$
$A_i$	The auctioneer who publishes task $T_i$ , where $i \in N$
$B_j$	The team $j$ who received auction message, i.e., the bidder, where $j \in M$
$u_i$	The utility for a bidder who completes task $T_i$ , where $i \in N$
$g_{ij}$	The net utility for bidder $B_j$ who completes task $T_i$ , which equals $u_i - c_{ij}$
$c_{ij}$	The cost of $B_j$ participating in task $T_i$ , where $i \in N$ and $j \in M$
$c'_{ij}$	The opportunity cost of $B_j$ participating in task $T_i$ , where $i \in N$ and $j \in M$
$t_{need}$	The time limit for completing rescue operations in each buried site
$n_i$	The number of teams required to complete task $T_i$ , which is related to $t_{need}$
$d_{ij}$	The distance between task $T_i$ and $B_j$ , where $i \in N$ and $j \in M$
$t_{ij}$	The time $B_j$ spent in rescue operation of task $T_i$ , where $i \in N$ and $j \in M$
$y_j$	The number of buried sites within the scope of cooperation
$l_j$	The number of available rescue teams within the scope of cooperation
$\lambda$	The coefficient of bid price, $\lambda \in (0, 1)$
$p_{ij}$	The bid on task $T_i$ , which is made by $B_j$

### 3.1. Auctioneers

Rescue teams who have detected a buried site within the search radius take on the role of auctioneers. Other teams who are not at work presently within the scope of cooperation take on the role of bidders. Auctioneer  $A_i$  first evaluates the buried depth of  $T_i$ , and the number of required rescue teams  $n_i$  associated with  $t_{need}$  is derived as

$$n_i = \left\lfloor \frac{v_{rubble}}{s_{rubble} \cdot t_{need}} + 0.5 \right\rfloor \tag{4}$$

When  $n_i > 1$ , auctioneer  $A_i$  sends a request for cooperation to the bidders through broadcasting. Bidders make bids on the tasks within the scope of cooperation. Auctioneer  $A_i$  receives the bids, and then determines the winning bids. The number of winning bids for task  $T_i$  shall be  $n_i - 1$ . There exists time limit  $t_l$  for each round of auction. A round of auction would terminate when the duration exceeds  $t_l$  or the request for cooperation is satisfied. If the number of winning bids for task  $T_i$  is less than  $n_i - 1$ , the rescue teams who win the bids would start rescue operations, the auctioneer  $A_i$  would start another round of auction, and the procedure repeats until the request for cooperation is satisfied. If the number of winning bids equals  $n_i - 1$ , the task allocation would be completed.

### 3.2. Bidders

The rescue teams who received auction messages take the role of bidders. Bidders would bid on only one task each time. When receiving more than one auction message, Bidders are supposed to choose the task which could bring about the most net utility to bid on. Let  $g_i$  be the net utility gained by bidder  $B_j$  who participate in task  $T_i$ , and  $g_i$  is formulated as  $u_i - c_{ij}$ , where  $u_i$  is the utility bidder  $B_j$  could gain from participating in task  $T_i$ ,  $c_{ij}$  is the cost of  $B_j$  participating in task  $T_i$ . If bidder  $B_j$  could gain the most net utility from task  $T_i$ ,  $B_j$  would bid on task  $T_i$  with the bid price  $p_{ij}$ . For each bidder, both the decision about which task to bid on and the bid price are variable until it is assigned with a particular task.

#### 3.2.1. The Utility Function of Bidders

The utility  $u_i$  bidders gain from task  $T_i$  indicates the task's rescuing priority. The more urgent the task is, the higher the utility would be. The utility  $u_i$  could be measured by buried depth, number of buried victims and severity of injury. In this paper, the utility is calculated through fuzzy comprehensive evaluation (FCE).

Let  $Z = \{z_1, z_2, \dots, z_q\}$  be the factor set, where  $z_a (a = 1, 2, \dots, q)$  denotes the a-th factor,  $q$  denotes the number of factors. Let  $V = \{v_1, v_2, \dots, v_p\}$  be the evaluation set, where  $v_b (b = 1, 2, \dots, p)$  denotes one evaluation level,  $p$  denotes the number of levels.

We calculate the membership degree of each factor to  $V$  according to membership function. For example, the membership degree of  $z_a$  is  $R_a = (r_{a1}, r_{a2}, \dots, r_{ap})$ , which is also called single factor evaluation set. The overall fuzzy evaluation matrix of all  $q$  factors is  $R = (R_1, R_2, \dots, R_q)'$ . Let  $W = (w_1, w_2, \dots, w_q)$  be the weight vector, where  $w_a$  denotes the relative importance of a-th factor. Consequently, the evaluation result would be

$$H = W \times R = (h_1, h_2, \dots, h_p) \tag{5}$$

When evaluating the utility of task  $T_i$ , we first calculate the comprehensive score of task  $T_i$   $U_i^T = \frac{\sum_{b=1}^p h_b \cdot v_b}{\sum_{b=1}^p h_b}$ , and then obtain the utility of task  $T_i$   $u_i = \frac{U_i^T}{n_i}$ .

### 3.2.2. The Cost of Bidders

In disaster relief, saving the cost should not be put in the first place. However, the cost we introduce in this paper does not refer to investment in equipment or manpower. The cost  $c_{ij}$  of bidder  $B_j$  involving in task  $T_i$  refers to the distance from  $B_j$  to  $T_i$ , and the time  $t_{ij}$  spent in rescue operation. By introducing the cost in this model, we can take the location of buried sites as a factor to determine the allocation of task, and reduce time spent in moving process.

The cost  $c_{ij}$  is a function of distance  $d_{ij}$  from  $B_j$  to  $T_i$  and the time  $t_{ij}$  spent in rescue operation.

$$c_{ij} = f(d_{ij}, t_{ij}) \tag{6}$$

When auctioneer  $A_i$  estimates the required number of rescue teams  $n_i$  as shown in Equation (4), the time  $t_{ij}$   $B_j$  spends in rescue operation is set to be approximately equal to  $t_{need}$ , and the same goes with all the other bidders. Therefore, the time spent in rescue operation does not make a difference, and it is ignored in the following model, i.e.,  $c_{ij} = f(d_{ij})$ .

When receiving more than one auction message, bidders are supposed to take opportunity cost  $c'_{ij}$  into consideration as to determine bid price  $p_{ij}$ . Opportunity cost  $c'_{ij}$  is the loss of net utility bidder  $B_j$  could gain from the second best choice  $T_s$  when choosing task  $T_i$  to bid on, as shown in Equation (7).

$$c'_{ij} = u_s - f(d_{sj}) \tag{7}$$

### 3.2.3. The Bidding Strategy of Bidders

When determining the bid price, in addition to utility  $u_i$ , cost  $c_{ij}$  and opportunity cost  $c'_{ij}$ , bidder  $B_j$  has to consider the number of buried sites within the scope of cooperation  $y_j$  and the number of available rescue teams within the scope of cooperation  $l_j$ . Let  $\rho_j = y_j/l_j$ , the larger the value of  $\rho_j$ , the more likely for  $B_j$  to be involved in a task. Therefore, in order to make as many tasks as possible to be assigned to enough rescue teams, a coefficient  $\lambda_j$  is introduced in this model to adjust bid price, as shown in Equation (8). The coefficient  $\lambda_j$  needs to be tuned when applied in different cases. The bid price  $p_{ij}$  is defined in Equation (9).

$$\lambda_j = 1 - \frac{\rho_j - \rho_{\min}}{\rho_{\max} - \rho_{\min}}, \quad \lambda_j \in (0, 1) \tag{8}$$

$$p_{ij} = \lambda_j(u_i - c_{ij} - c'_{ij}) \tag{9}$$

### 3.3. The Adjustment in Task Allocation

When bidder  $B_j$  is participating in task  $T_i$ , the utility  $u_i$  it could gain from task  $T_i$  varies as time goes by. Assuming that a new task  $T_k$  is auctioned around  $B_j$ , and there exist few available rescue teams for task  $T_k$  within the scope of cooperation  $s_c$ . Then  $B_j$  would evaluate task  $T_k$ . If the net utility  $g_{kj}$  of task  $T_k$  were much higher than  $g_{ij}$  of task  $T_i$ , i.e.,  $g_{kj} - g_{ij} \geq Q$  ( $Q$  is pre-defined), the current allocation of tasks would be revised. The number of teams required to complete task  $T_i$  would be updated according to Equation (4), for the buried depth  $v_{rubble}$  is changing. The updated number of required teams for  $T_i$  is  $n'_i (n'_i \leq n_i)$ , then auctioneer  $A_i$  would allow up to  $n^b_i = n_i - n'_i$  bidders to withdraw from task  $T_i$ . Assuming task  $T_k$  still lacks  $n^c_k$  available rescue teams within the scope of cooperation, then the number of rescue teams that withdraw from task  $T_i$  would be  $\min(n^b_i, n^c_k)$ . The rescue teams that withdraw from  $T_i$  would bid on new task  $T_k$ .

### 4. Simulation Results

#### 4.1. Experimental Settings

The search and rescue in landslide disaster are simulated here to evaluate the performance of proposed rescue plan. The simulation is implemented in NetLogo. The affected area is characterized as a circular area of radius 100 m, assuming that there are 100 victims and 20 rescue teams in this area. The victims are located in randomly-distributed buried sites. The unit of simulation steps is minute. A round of simulation would continue until all survivors get rescued, and the time limit of one round of simulation is set to be 72 h, i.e., 4320 simulation steps.

According to the records of casualties in landslide over the last decade, the proportions of four kinds of injury severities in each scenario are assumed in Table 2.

**Table 2.** The proportions of four injury severities in each scenario.

Injury Severity	Scenarios		
	Fatal (%)	Serious (%)	Normal (%)
Death	40	30	20
Heavy injury	30	25	20
Slight injury	10	15	20
No injury	20	30	40

The settings of simulation are as follows: the number of buried survivors in one single buried site  $\beta_i \sim U(1, 3)$ ; the injury severity of victims  $v_{si}$  is initialized according to Table 2; the buried depth  $v_{rubble} \sim N(120, 30)$ ; the time limit for completing rescue operations in each buried site  $t_{need} = 30$ ; the number of rescue teams  $m = 20$ ; search speed  $3 \text{ m/min}$ ; search radius  $s_r = 3 \text{ m}$ ; speed of rescue  $s_{rubble} = 0.5$ ; move lengths  $s_l$  are determined through Equation (3), in which  $\mu = 2$ ; maximum turning angle  $s_a = \pi$ , i.e., turning angles  $s_\theta \sim U(0, \pi)$ ; If there are survivors trapped in a buried site within the search radius, rescue teams are able to locate the buried site with a probability  $prob = 20\%$ ; scope of cooperation  $s_c = 40 \text{ m}$ ; the time limit for each round of auction  $t_l = 3 \text{ min}$ .

When making bids on tasks, bidders would evaluate the utility of tasks through FCE. The factor set  $Z = \{Buried \text{ Depth}, Number \text{ of Victims}, Total \text{ Injury Severity}\}$ . Buried depth indicates the workload of rescue. Number of victims refers to the number of victims who are buried in this buried site. The injury severities are coded as “0”, “3”, “2” and “1”, corresponding to “death”, “heavy-injury”, “slight-injury” and “no-injury”. Total injury severities are the sum of injury severities of victims buried here. The weight vector of three factors in FCE  $W = (1/3, 1/3, 1/3)$ . Evaluation criterions are shown in Table 3.

**Table 3.** Evaluation criterion of tasks’ urgency levels.

	Urgent	Less Urgent	Normal
Buried depth	150	120	90
Number of victims	3	2	1
Total injury severity	9	5	1

The evaluation set  $V = \{Urgent, Less \text{ Urgent}, Normal\}$ , shown in Table 3. The membership degree of factor  $z_a$  to evaluation level  $v_b$ , denoted as  $r_{ab}$ , is calculated through semi-trapezoid distribution function. For example, the membership degree of buried depth to  $v_1$  is calculated by Equation (10).

$$r_{11} = \begin{cases} 1 & v_{rubble} \geq 150 \\ \frac{v_{rubble}-120}{30} & 120 < v_{rubble} < 150 \\ 0 & v_{rubble} \leq 120 \end{cases} \quad (10)$$

The model outputs a number of comparative statistics at the end of a simulation, which include: survival probability of each victim  $v_{sp}$ , average survival probability  $\bar{p}_s$ , relative survival probability  $\bar{p}_{rs}$ , ratio of survivors getting rescued  $\bar{p}_r$  and average elapsed time for one site getting rescued  $\bar{t}_a$ .

Survival probabilities  $v_{sp}$  of victims are related to their injury severity  $v_{si}$ . Without timely rescue, the health condition of a victim could deteriorate continuously. Survival probability  $v_{sp}$  is assumed to deteriorate with time until the victim gets rescued. In this paper, three curves are adopted to estimate survival probability for different injury severity [24].

$$\begin{aligned} v_{sp\text{-hi}} &= e^{-(t/3.324)^{3.71}} \\ v_{sp\text{-si}} &= e^{-(t/26.59)^{3.71}} \\ v_{sp\text{-ni}} &= e^{-(t/66.48)^{3.71}} \end{aligned} \tag{11}$$

where  $v_{sp\text{-hi}}$  denotes survival probability of victims who are heavily injured,  $v_{sp\text{-si}}$  denotes survival probability of victims who are slightly injured, and  $v_{sp\text{-ni}}$  denotes survival probability of victims who are not injured.  $t$  denotes trapped time (h). Three curves, shown in Figure 4, from left to right, represent survival probability of victims with heavy injury, slight injury and no injury, respectively.

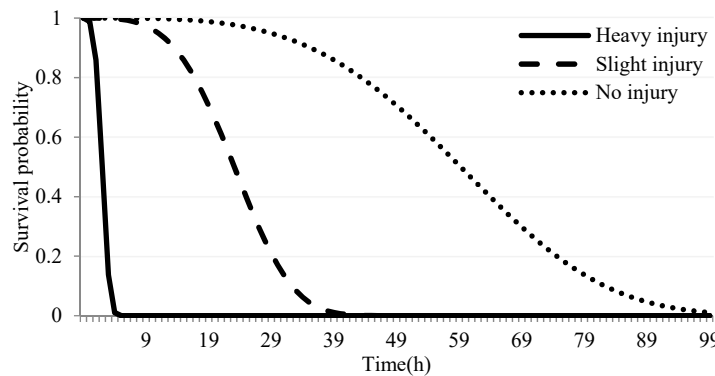


Figure 4. The deterioration rate of survival probabilities of victims with different injury severity.

Relative survival probability  $\bar{p}_{rs}$  is the ratio of average survival probability to initial average survival probability. When disaster happens, there always exist some survivors under the rubbles. Some of them would be rescued, and some of them would die without timely rescue,  $\bar{p}_r$  is the ratio of survivors getting rescued in the end. In the rescuing process, a lot of time is required until one site gets rescued, and  $\bar{t}_a$  is the average required time.

#### 4.2. Results

Simulations are run in three scenarios, including “fatal”, “serious” and “normal”, and the simulation results of cooperative rescue plan would be compared with non-cooperative rescue plan. In non-cooperative rescue plan, rescue teams only rescue the victims which are detected by themselves. Each simulation is repeated 200 times. The simulation results are analyzed through three output indicators, i.e., relative survival probability  $\bar{p}_{rs}$  (the initial relative survival probability is 1), ratio of survivors getting rescued  $\bar{p}_r$  and average elapsed time for one site getting rescued  $\bar{t}_a$ , shown in Table 4. The comparison shows that the auction-based cooperative rescue plan outperforms non-cooperative rescue plan in three scenarios at 1% significance level, which can be seen from the independent-samples  $t$  test in Table 4.

**Table 4.** The comparison of simulation results in three scenarios.

		$\bar{p}_{rs}$ (%)	$\bar{p}_r$ (%)	$\bar{t}_a$ (min)
Fatal	Cooperation	56.40	64.62	512.2
	No-cooperation	48.96	57.22	653.2
	<i>t</i> test	7.44 ***	7.40 ***	−141.0 ***
Serious	Cooperation	68.17	75.11	587.0
	No-cooperation	62.37	69.04	703.6
	<i>t</i> test	5.80 ***	6.07 ***	−116.6 ***
Normal	Cooperation	76.26	82.15	624.1
	No-cooperation	71.30	78.01	749.0
	<i>t</i> test	4.96 ***	4.14 ***	−124.9 ***

Note: “\*”, “\*\*”, “\*\*\*” denote that the tests are significant at significance level 0.1, 0.05, 0.01, respectively.

The simulation of cooperative rescue plan is repeated 200 times in three scenarios separately. The average relative survival probability and average ratio of rescued victims of 200 runs at every simulation step are depicted in Figures 5–7.

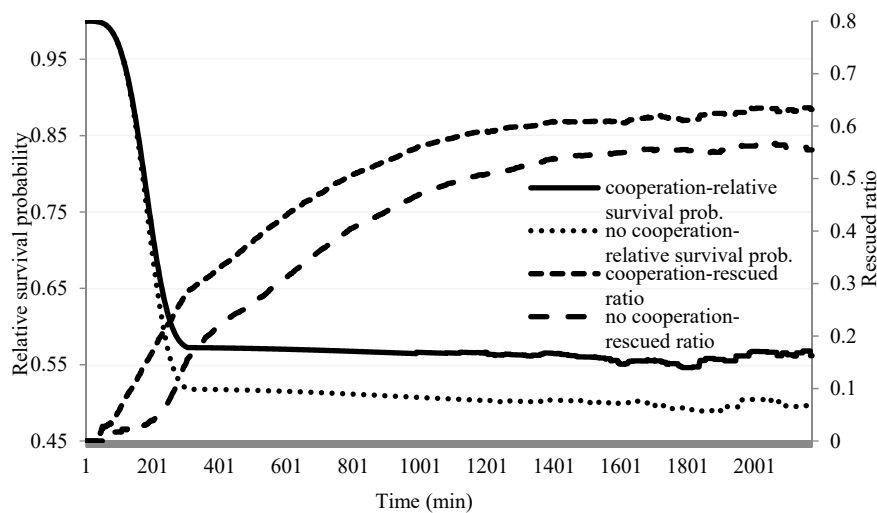


**Figure 5.** The average output results of 200 runs at every step in scenario “Fatal”.

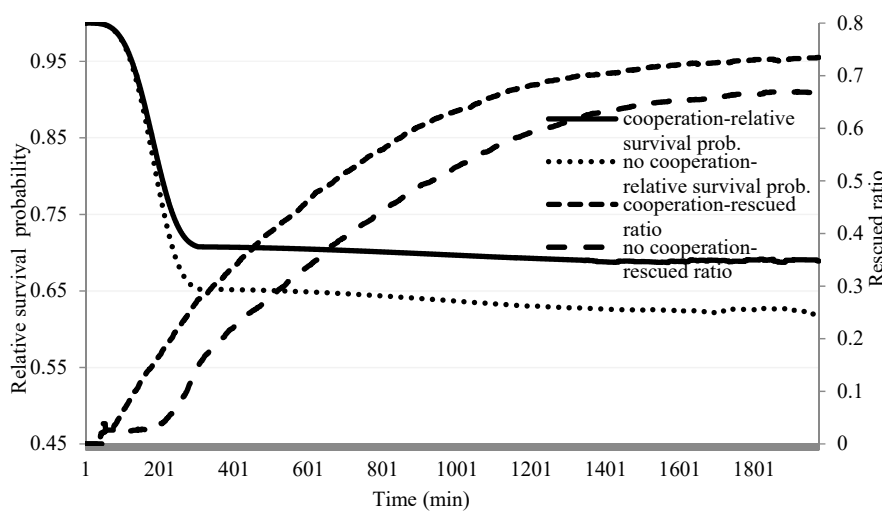


**Figure 6.** The average output results of 200 runs at every step in scenario “Serious”.

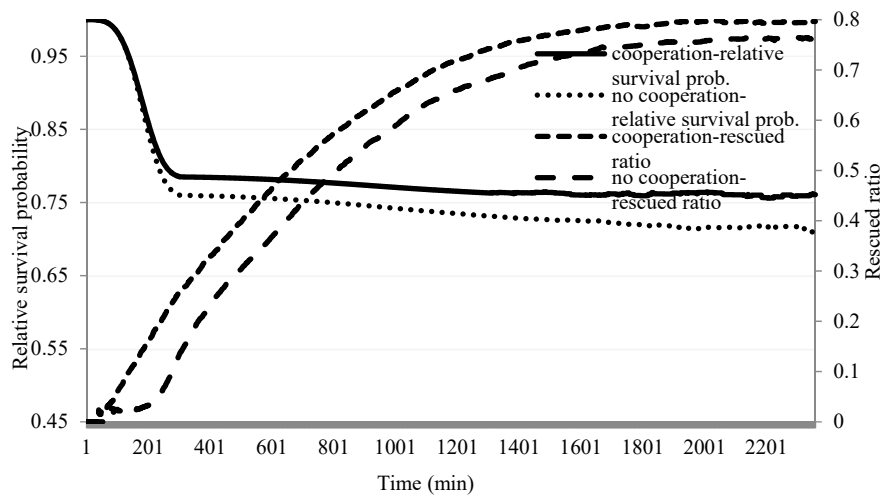


**Figure 7.** The average output results of 200 runs at every step in scenario “Normal”.

In Figures 5–7,  $x$ -axis indicates the simulation step, which is also the time in the process of disaster relief. The primary  $y$ -axis indicates relative survival probability, and the secondary  $y$ -axis indicates ratio of rescued victims. As can be seen from the three figures, relative survival probability under auction-based cooperative rescue plan remains higher than non-cooperative rescue plan at every step in the simulation. Relative survival probability decreases rapidly in the beginning, because of the existence of victims who are heavily injured, and their survival probability decrease extremely rapidly, as shown in Figure 4. When rescue lasts for about 300 min, the decrease of relative survival probability would slow down. Because the victims who are heavily injured would die if not rescued within 300 min, there exist only victims who are slightly injured or not injured, whose survival probability decrease slowly.

The simulation results indicate that the cooperative rescue plan would improve the rescue result a lot, compared with the non-cooperative rescue plan. In the above three scenarios, it increases victims’ relative survival probability by 7–15%, increases the ratio of survivors getting rescued by 5.3–12.9%, and decreases the average elapsed time for one site getting rescued by 16.6–21.6%. Moreover, as the scenario worsens, the improvement would be more significant generally.

#### 4.3. Verification and Validation

The verification and validation is one of the common critical issues in agent-based simulation, and it is indeed a difficulty in this area. This is because such computational systems or simulations are difficult to verify in terms of checking program-bugs and their outcomes are also difficult to validate even when there are no program-bugs [31].

We have adopted a bottom-up approach to model the search and rescue (SAR). Different from physical phenomena, we cannot experience landslides repeatedly to collect data that show some relationship between the parameters of rescue operations and the rescue efficiency [23]. Thus we had interviewed some first responders and experts who specialize in on-site search and rescue for advice before we built the conceptual model. We built the model step by step, and at each step, we will check the logic and internal relationships to guarantee its reasonability. Therefore, we can ensure that the assumptions, logic, and casual relationships in the conceptual model are reasonable, and the model is an adequate conceptualization of the real world [32].

It is important to validate whether or not the results from the virtual experiments match the results from the real world. However, we can hardly find a complete record of a landslide. Thus we will validate it mainly through experts’ knowledge and experience. We have conducted a large number of repetitions of the simulation, evaluated the simulation through robustness analysis and sensitivity

analysis, and the simulation results could match the results from experts’ experience. Therefore, this model is verified and valid to a certain degree.

Moreover, we have calculated the relative error  $\delta$  of three indicators in three scenarios, shown in Table 5. Relative error measures the relative difference between an individual value and the true value (or average value).

**Table 5.** The relative error of three indicators in three scenarios.

		$p_{rs}$	$p_r$	$t_a$
Fatal	Cooperation	7.5%, [0.7%, 16.2%]	6.9%, [0.5%, 14.9%]	8.7%, [0.8%, 20.3%]
	No-cooperation	10.3%, [0.8%, 23.9%]	9.4%, [0.3%, 24.4%]	8.6%, [0.9%, 20.5%]
Serious	Cooperation	5.8%, [0.8%, 13.8%]	5.6%, [0.6%, 14.4%]	8.2%, [0.7%, 20.7%]
	No-cooperation	6.6%, [0.2%, 16.1%]	5.9%, [0.5%, 15.2%]	6.8%, [0.4%, 17.1%]
Normal	Cooperation	4.4%, [0.2%, 10.7%]	3.4%, [0.2%, 8.5%]	6.5%, [0.8%, 17.0%]
	No-cooperation	4.6%, [0.4%, 12.5%]	4.7%, [0.4%, 12.1%]	6.1%, [0.5%, 15.1%]

Table 5 shows the mean relative error and the interval in which 90% of the sample’s relative error falls. For instance, the mean relative error of  $p_{rs}$  under cooperative rescue plan in scenario “Fatal” is 7.5%, and 90% of the relative error of  $p_{rs}$  falls in interval [0.7%, 16.2%]. As can be seen from Table 5, the mean relative error of three indicators in three scenarios ranges from 3 to 10%. The results show that the relative error in our simulation is maintained at a low level, which means our simulation is quite stable. We can be sure that our simulation results have reflected system behavior and not simulation errors.

### 5. Analytical Evaluation

Let  $E$  be the evaluation indicator, and it is formulated as  $E = \frac{\bar{p}_r + \bar{p}_{sr}}{2}$ , where  $\bar{p}_{rs}$  is the relative survival probability, and  $\bar{p}_r$  is the ratio of rescued victims, thus  $E \in [0, 1]$ . The larger the value of  $E$ , the more effective the rescue plan. The evaluation indicator  $E$  also represents the rescue efficiency in the following robustness analysis and sensitivity analysis.

#### 5.1. Robustness Analysis

We present the robustness analysis here in order to consider not only the rescue efficiency of cooperative rescue plan under normal conditions, but also the reliability under extreme operative situations. In the robustness analysis, a series of simulations have been executed to measure the rescue plan’s adaptability to unexpected situations. Let  $LRS$  be an indicator to measure robustness of the model [33], shown in Equation (12).

$$LRS = \frac{\sum (x_i - \bar{x}_i)(E_i - \bar{E}_i)}{\sum (x_i - \bar{x}_i)^2} \tag{12}$$

where  $x_i$  ( $i = 1, 2, 3 \dots$ ) denotes specified values of the parameter that we have considered for variations,  $E_i$  denotes the corresponding rescue efficiency,  $\bar{x}_i$  and  $\bar{E}_i$  denote the average values. The more significant the  $LRS$  is, the less robust the model becomes, and vice versa.

The parameters that we have considered for variations in robustness analysis are search radius  $s_r$  and scope of cooperation  $s_c$ . Search radius could decrease for severe visibility conditions. Scope of cooperation could be affected by extreme operating environment and severe communication conditions.

In Figure 8,  $x$ -axis denotes independent variables, i.e., the parameters that have considered for variations, and  $y$ -axis denotes dependent variables. We have explored the impact of varying search radius from 3 m to 8.1 m with an interval of 0.3 m; the scope of cooperation from 5 m to 125 m with an interval of 5 m. For every case described here, the simulation was repeated 200 times.

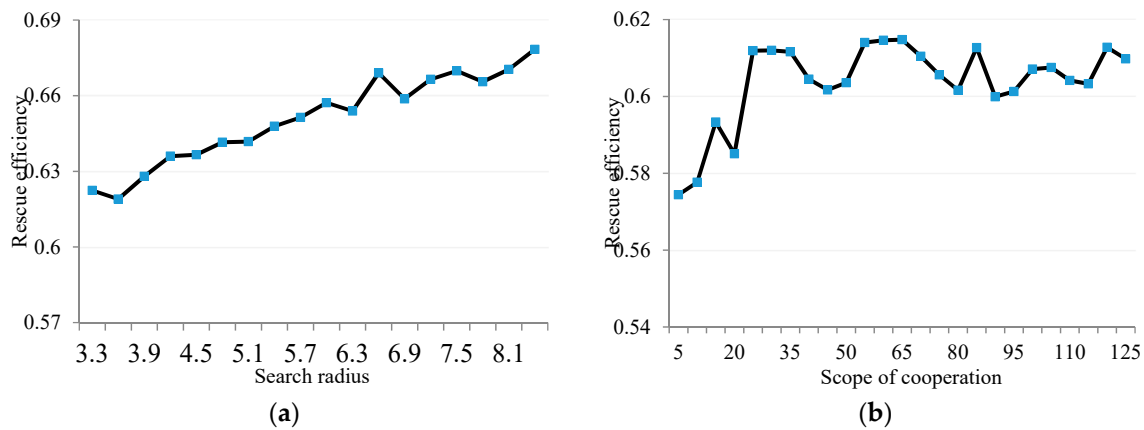


**Figure 8.** Robustness analysis of cooperative rescue plan. (a) Effect of search radius on rescue efficiency; (b) Effect of cooperation scope on rescue efficiency.

The results of robustness analysis show a number of interesting and reasonable dynamics. As the search radius increases, the rescue efficiency improves significantly, as shown in Figure 8a. When the rescue operations occur in the night, the search radius would decrease for low visibility, resulting in the lowering of rescue efficiency. The correlation between search radius and rescue efficiency is significant at 1% significance level, and the indicator  $LRS$  is 0.011, which indicates that rescue efficiency is easily affected by the variation of visibility conditions.

As can be seen from Figure 8b, the rescue efficiency does not show a regular change with the scope of cooperation  $s_c$ , especially when  $s_c$  is larger than 20 m, the rescue efficiency changes very little, and falls in [0.60, 0.615] basically. When the scope of cooperation is small, rescue teams' request for cooperation cannot be satisfied. However, as the scope of cooperation  $s_c$  increases to  $\hat{s}_c = 25$  m, the cooperation could be reached within a short time. When  $s_c$  is larger than 20 m, the indicator  $LRS$  is  $-3.6 \times 10^{-5}$ , indicating no correlation between rescue efficiency and scope of cooperation. To summarize, when  $s_c$  falls in [5 m, 20 m], it is not easy to reach cooperation, and the increase of  $s_c$  could result in improvement in rescue efficiency. When  $s_c$  falls in [25 m, 125 m], the increase of  $s_c$  does not make a difference to the rescue efficiency, i.e., the cooperative rescue plan is reliable on the condition that scope of cooperation is larger than a threshold.

## 5.2. Sensitivity Analysis

We present the sensitivity analysis here in order to test how much the simulation results could be affected by the variation of parameters, which reflects the sensitivity of the rescue plan to some parameters. The sensitivity is tested by varying the time limit for completing rescue operations in each buried site  $t_{need}$  from 10 min to 125 min with an interval of 5 min; the maximum turning angle  $s_a$  from  $\pi/6$  to  $2\pi$  with an interval of  $\pi/12$ . For every case described here, the simulation was repeated 200 times.

The time limit for completing rescue operations in each buried site  $t_{need}$  is used to estimate the number of teams required to complete a task  $n_i$ , shown in Equation (4), the increase of  $t_{need}$  would lead to decrease of  $n_i$ . As can be seen from Figure 9a, the rescue efficiency has shown a regular change with the time limit for completing rescue operations in each buried site  $t_{need}$ . As  $t_{need}$  increases, the rescue efficiency improves significantly, but when  $t_{need}$  is larger than  $\hat{t}_{need} = 30$  min, the rescue efficiency lowers with the increase of  $t_{need}$ . When  $t_{need}$  is less than  $\hat{t}_{need}$ , the number of teams required to complete a task  $n_i$  would be huge, so a large number of rescue teams should be transferred here. As a result, all the rescue teams would spend a lot of time on the roads, and spare little time on independent search, which leads to high cost of cooperation and low rescue efficiency. When  $t_{need}$  is larger than  $\hat{t}_{need}$ , the number of teams required to complete a task  $n_i$  would be small, which makes the cooperative

behavior hardly seen between rescue teams. Without enough cooperation, the rescue efficiency lowers significantly, and the result would worsen when  $t_{need}$  gets larger and larger. The relationship between  $t_{need}$  and rescue efficiency is fitted with a quadratic function, as can be seen from Figure 9a, and the R-squared statistic is 0.7552. The optimal value  $\hat{t}_{need}$  can be derived from the fitting function, and  $\hat{t}_{need}$  is 30 min in our given case. The above analysis shows that there exist a trade-off between cooperation and independent search; we always need to find the appropriate  $t_{need}$  to ensure the high rescue efficiency.

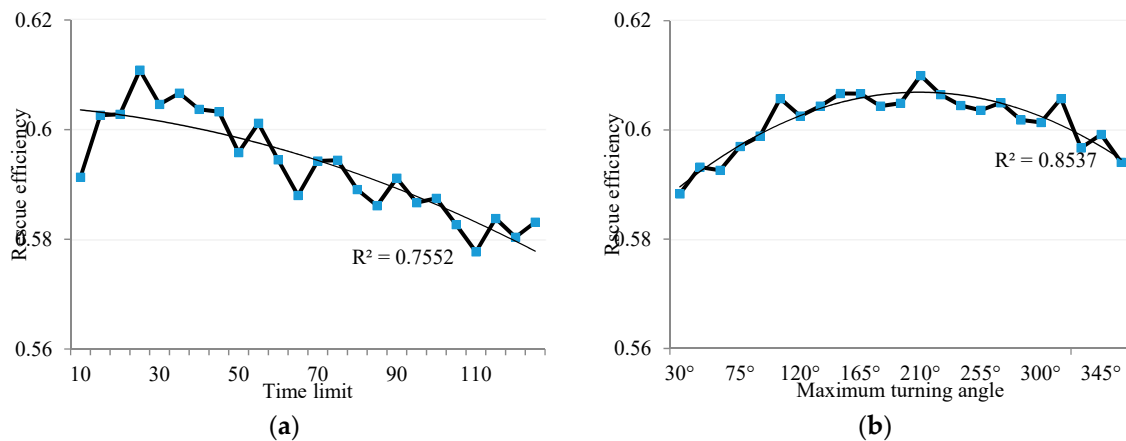


**Figure 9.** Sensitivity analysis of cooperative rescue plan. (a) Relation between the time limit for rescuing one site and rescue efficiency; (b) Relation between the maximum turning angle and rescue efficiency.

The relationship between maximum turning angle  $s_a$  and rescue efficiency is depicted in Figure 9b. When  $s_a$  is less than  $\hat{s}_a$ , the rescue efficiency is low and it improves with the increase of  $s_a$ . Because  $s_a$  is small, the range of search angle would be limited. Thus, a new position is most likely generated at the same direction as in the previous step, and the search trajectory is like a straight line, which makes the search coverage incomplete. When  $s_a$  is larger than  $\hat{s}_a$ , the rescue efficiency lowers with the increase of  $s_a$ . The large value of  $s_a$  would lead to a wide range of search angle, and too wide a range would result in aimlessness. Rescue teams might spend a large amount of time searching the same area, resulting in low efficiency, and the results would worsen when  $s_a$  gets larger and larger. The relationship between  $s_a$  and rescue efficiency is also fitted with a quadratic function, and the R-squared statistic is 0.8537. The optimal value  $\hat{s}_a$  is approximately equal to  $2\pi/3$  in our given case. To summarize, there exists a trade-off between directional moves and search coverage, and we need to balance them and find the appropriate range of the turning angle.

## 6. Conclusions

This paper aims to use an auction-based task allocation scheme to develop a cooperative rescue plan, and optimize it through agent-based simulation, which could fully cope with dynamics and complexities of disaster relief. The disaster search has been integrated with cooperative rescue in this paper. The proposed cooperative rescue plan outperforms the non-cooperative rescue plan with respect to rescue efficiency in three scenarios. The robustness analysis shows that the search radius could affect rescue efficiency significantly, thus we could adjust investments in equipment to increase search radius, bringing about improvement in rescue efficiency. It is necessary that the scope of cooperation should be kept larger than a threshold, thus the rescue teams' request for cooperation can be satisfied and the rescue efficiency can be maintained at a high level. The sensitivity analysis shows that there exist optimal values for both the time limit for completing rescue operations in each buried site and the maximum turning angle. The determination of optimal value is a trade-off, and we need to find the optimal value for  $t_{need}$  and  $s_a$  based on actual conditions of disaster environments, which could lead to

a great improvement in rescue efficiency. In the future work, we will characterize the rescue teams by specific functions, and study the rescue cooperation between different functional rescue teams.

The parameter calibration is a challenge and a critical issue in modeling and simulation work. However, we can hardly find a complete record of a landslide. Some parameters cannot be retrieved from historical data in our simulation, as they are either missing or not recorded. The data scarcity has limited the classical approaches to calibrate model parameters [34]. One approach to overcome the limitation of sparse calibration data is to use additional data sources to calibrate model parameter sets. Another promising strategy is to break down the model into smaller sub-models, and the sub-models are calibrated separately [34,35]. The approach proposed by Liu et al. [36] may fit well in our case for the similarity between the two cases. This approach could reduce the effects on calibration brought by data scarcity to a certain degree, but a lot of samples (input-output pairs) are needed in this approach. In our research, we have not got enough records currently, and thus we set the parameter and calibrate it through the empirical data from experienced staff. Certainly the calibration in our work is not enough. In the future, we will collect a large number of records in reality, and calibrate the parameters under data scarcity with the idea described in Liu's work [36].

**Acknowledgments:** This work was supported by National Natural Science Foundation of China (grant numbers 71473232, 71573237); Research Foundation of Humanities and Social Sciences of Ministry of Education of China (grant number 15YJA630019); and the Fundamental Research Funds for National University, China University of Geosciences (Wuhan) (grant number 1610491T12).

**Author Contributions:** Kejun Zhu conceived and designed the experiments; Jian Tang and Can Liao performed the experiments; Haixiang Guo and Shuwen Zhang analyzed the data; Jian Tang wrote the paper.

**Conflicts of Interest:** The authors declare no conflict of interest.

## References

1. Campbell, A.M.; Jones, P.C. Prepositioning supplies in preparation for disasters. *Eur. J. Oper. Res.* **2011**, *209*, 156–165. [[CrossRef](#)]
2. Sheu, J. Dynamic relief-demand management for emergency logistics operations under large-scale disasters. *Res. Part E Logist. Transp. Rev.* **2010**, *46*, 1–17. [[CrossRef](#)]
3. Gan, H.; Richter, K.; Shi, M.; Winter, S. Integration of simulation and optimization for evacuation planning. *Simul. Model. Pract. Theory* **2016**, *67*, 59–73. [[CrossRef](#)]
4. Zhang, M.; Zhang, B.; Zheng, Y. Bio-Inspired Meta-Heuristics for Emergency Transportation Problems. *Algorithms* **2014**, *7*, 15–31. [[CrossRef](#)]
5. Zheng, Y.; Chen, S.; Ling, H. Evolutionary optimization for disaster relief operations: A survey. *Appl. Soft Comput.* **2015**, *27*, 553–566. [[CrossRef](#)]
6. Nadi, A.; Edrisi, A. Adaptive multi-agent relief assessment and emergency response. *Int. J. Dis. Risk Reduct.* **2017**, *24*, 12–23. [[CrossRef](#)]
7. Bilbao, M.N.; Del Ser, J.; Perfecto, C.; Salcedo-Sanz, S.; Portilla-Figueras, J.A. Cost-efficient deployment of multi-hop wireless networks over disaster areas using multi-objective meta-heuristics. *Neurocomputing* **2018**, *271*, 18–27. [[CrossRef](#)]
8. Liang, H.; Kang, F. A novel task optimal allocation approach based on Contract Net Protocol for Agent-oriented UUV swarm system modeling. *Opt.-Int. J. Light Electron Opt.* **2016**, *127*, 3928–3933. [[CrossRef](#)]
9. Su, X.; Zhang, M.; Ye, D.; Bai, Q. In A dynamic coordination approach for task allocation in disaster environments under spatial and communicational constraints. In Proceedings of the AAAI Workshop on Multiagent Interaction without Prior Coordination, Quebec City, QC, Canada, 27–28 July 2014; p. 7.
10. Ju, C.; Chen, T. Extended labor division model of ant colony based on ability-evaluation and interest-driven and its applications in dynamic task allocations. *Syst. Eng. Theory Pract.* **2014**, *34*, 84–93.
11. Liu, C.; Kroll, A. Memetic algorithms for optimal task allocation in multi-robot systems for inspection problems with cooperative tasks. *Soft Comput.* **2015**, *19*, 567–584. [[CrossRef](#)]
12. Bilbao, M.N.; Ser, J.D.; Salcedo-Sanz, S.; Casanova-Mateo, C. On the application of multi-objective harmony search heuristics to the predictive deployment of firefighting aircrafts: A realistic case study. *Int. J. Bio-Inspir. Comput.* **2015**, *7*, 270–284. [[CrossRef](#)]

13. Landatorres, I.; Manjarres, D.; Bilbao, S.; Ser, J.D. Underwater Robot Task Planning Using Multi-Objective Meta-Heuristics. *Sensors* **2017**, *17*, 762. [[CrossRef](#)] [[PubMed](#)]
14. Nanjanath, M.; Erlandson, A.J.; Andrist, S.; Ragipindi, A.; Mohammed, A.A.; Sharma, A.S.; Gini, M. Decision and Coordination Strategies for RoboCup Rescue Agents. In Proceedings of the International Conference on Simulation, Modeling, and Programming for Autonomous Robots, Darmstadt, Germany, 15–18 November 2010; Springer: Berlin/Heidelberg, Germany, 2010; pp. 473–484.
15. Nair, R.; Ito, T.; Tambe, M.; Marsella, S. Task allocation in the robocup rescue simulation domain: A short note. In *Robot Soccer World Cup*; Springer: Berlin/Heidelberg, Germany, 2001; pp. 751–754.
16. Kong, Y.; Zhang, M.; Ye, D. A Group Task Allocation Strategy in Open and Dynamic Grid Environments. In *Recent Advances in Agent-Based Complex Automated Negotiation*; Fukuta, N., Ito, T., Zhang, M., Fujita, K., Robu, V., Eds.; Springer: Basel, Switzerland, 2016; pp. 121–139.
17. Smith, R.G. The Contract Net Protocol: High-Level Communication and Control in a Distributed Problem Solver. *IEEE Trans. Comput.* **1980**, *C-29*, 1104–1113.
18. Chen, J.; Sun, D. Coalition-Based Approach to Task Allocation of Multiple Robots with Resource Constraints. *IEEE Trans. Autom. Sci. Eng.* **2012**, *9*, 516–528. [[CrossRef](#)]
19. Ramchurn, S.D.; Farinelli, A.; Macarthur, K.S.; Jennings, N.R. Decentralized Coordination in RoboCup Rescue. *Comput. J.* **2010**, *53*, 1447–1461. [[CrossRef](#)]
20. D’Uffizi, A.; Simonetti, M.; Stecca, G.; Confessore, G. A Simulation Study of Logistics for Disaster Relief Operations. *Procedia CIRP* **2015**, *33*, 157–162. [[CrossRef](#)]
21. Duguay, C.; Chetouane, F. Modeling and Improving Emergency Department Systems using Discrete Event Simulation. *Simul. Trans. Soc. Model. Simul. Int.* **2007**, *83*, 311–320. [[CrossRef](#)]
22. Buford, J.; Jakobson, G.; Lewis, L. Multi-agent situation management for supporting large-scale disaster relief operations. *Int. J. Intell. Control Syst.* **2006**, *11*, 284–295.
23. Takahashi, T.; Tadokoro, S.; Ohta, M.; Ito, N. Agent based approach in disaster rescue simulation—from test-bed of multiagent system to practical application. In *RoboCup: Robot Soccer World Cup V*; Springer: Berlin/Heidelberg, Germany, 2002; pp. 102–111.
24. Tani, A.; Yamamura, T.; Waridashi, Y.; Kawamura, H.; Takizawa, A. In Simulation on Rescue in Case of Earthquake Disaster by Multi-Agent System. In Proceedings of the 13th World Conference on Earthquake Engineering, Vancouver, BC, Canada, 1–6 August 2004.
25. Wosniack, M.E.; Santos, M.C.; Raposo, E.P.; Viswanathan, G.M.; Da Luz, M.G.E. Robustness of optimal random searches in fragmented environments. *Phys. Rev. E* **2015**, *91*. [[CrossRef](#)] [[PubMed](#)]
26. Cao, M.; Meng, Q.; Luo, B.; Zeng, M. Experimental comparison of random search strategies for multi-robot based odour finding without wind information. *Austrian Contrib. Vet. Epidemiol.* **2015**, *8*, 43–50.
27. Rhee, I.; Shin, M.; Hong, S.; Lee, K.; Kim, S.J.; Chong, S. On the Levy-Walk Nature of Human Mobility. *IEEE/ACM Trans. Netw.* **2011**, *19*, 630–643. [[CrossRef](#)]
28. Cabrera, E.; Taboada, M.; Iglesias, M.L.; Epelde, F.; Luque, E. Optimization of Healthcare Emergency Departments by Agent-Based Simulation. *Procedia Comput. Sci.* **2011**, *4*, 1880–1889. [[CrossRef](#)]
29. Nolting, B.C. Random Search Models of Foraging Behavior: Theory, Simulation, and Observation. Ph.D. Thesis, University of Nebraska, Lincoln, NE, USA, 2013.
30. Reynolds, A.M. Balancing the competing demands of harvesting and safety from predation: Lévy walk searches outperform composite Brownian walk searches but only when foraging under the risk of predation. *Phys. A Stat. Mech. Appl.* **2010**, *389*, 4740–4746. [[CrossRef](#)]
31. Takadama, K.; Suematsu, Y.L.; Sugimoto, N.; Nawa, N.E.; Shimohara, K. *Towards Verification and Validation in Multiagent-Based Systems and Simulations: Analyzing Different Learning Bargaining Agents*; Springer: Berlin/Heidelberg, Germany, 2003; pp. 26–42.
32. Sargent, R.G. Verification and validation of simulation models. *J. Simul.* **2013**, *7*, 12–24. [[CrossRef](#)]
33. Farinelli, A.; Grisetti, G.; Iocchi, L.; Lo Cascio, S.; Nardi, D. Design and evaluation of multi agent systems for rescue operations, Intelligent Robots and Systems. In Proceedings of the IEEE/RSJ International Conference on Intelligent Robots and Systems (IROS 2003), Las Vegas, NV, USA, 27–31 October 2003; pp. 3138–3143.
34. Rödiger, T.; Geyer, S.; Mallast, U.; Merz, R.; Krause, P.; Fischer, C.; Siebert, C. Multi-response calibration of a conceptual hydrological model in the semiarid catchment of Wadi al Arab, Jordan. *J. Hydrol.* **2014**, *509*, 193–206. [[CrossRef](#)]

35. Fehler, M.; Puppe, F. Approaches for resolving the dilemma between model structure refinement and parameter calibration in agent-based simulations. In Proceedings of the Fifth International Joint Conference on Autonomous Agents and Multiagent Systems, Hakodate, Japan, 8–12 May 2006; pp. 120–122.
36. Liu, Z.; Rexachs, D.; Epelde, F.; Luque, E. A simulation and optimization based method for calibrating agent-based emergency department models under data scarcity. *Comput. Ind. Eng.* **2017**, *103*, 300–309. [[CrossRef](#)]



© 2017 by the authors. Licensee MDPI, Basel, Switzerland. This article is an open access article distributed under the terms and conditions of the Creative Commons Attribution (CC BY) license (<http://creativecommons.org/licenses/by/4.0/>).